Naringenin Modulates Sertoli Cell Dysfunction and Altered SCF/c-kit Ligand System in the Setting of Combination Antiretroviral Therapy

Misturah Yetunde Adana[1,2], Edidiong Nnamso Akang[1,3], Offor Ugochukwu[1,4], Simeon Eche[5], Edwin Coleridge Stephen Naidu[1], Onyemaechi Okpara Azu[1,6]

[1] Discipline of Clinical Anatomy, School of Laboratory Medicine and Medical Sciences, University of KwaZulu-Natal, Durban, South Africa
[2] Department of Anatomy, Faculty of Basic Medical Sciences, College of Health Sciences, University of Ilorin, P.M.B. 1515 Ilorin, Nigeria
[3] Andrology unit, University of Pittsburg Medical Center Magee Women's Hospital, United States
[4] Department of Anatomy, Queen Mary University of London, Malta Campus, Mile End Road, London E1 4NS
[5] Genomics Unit, School of Laboratory Medicine and Medical Sciences, University of KwaZulu-Natal, Durban, South Africa
[6] Department of Medical Biosciences, University of the Western Cape, South Africa

Corresponding Author: Adana M.Y

Email: adana.my@unilorin.edu.ng, Tel. No.: +2348033727625

ABSTRACT

Combination Antiretroviral Therapy (cART) has been shown in previous studies to induce histopathological changes in the testes. An essential function of the c-kit signalling system is to control cell survival, proliferation, differentiation, and death. Consequently, certain male infertility may be explained by deregulating the SCF/c-kit system by attenuating or overactivating its signaling strength. This study examined the effects of antiretroviral drugs and a bioactive flavonoid, Naringenin on testicular ultrastructure, function and the SCF/c-kit ligand system. Six groups of five Sprague Dawley rats were assigned into cART (H), distilled water (DW), naringenin 40 mg/kg (N40), naringenin 80 mg/kg (N80), cART+naringenin 40 mg/kg (HN40), and cART+naringenin 80 mg/kg (HN80). Electron microscopy was employed to study testicular ultrastructural changes. The expressions of intratesticular SCF and c-kit mRNA were evaluated using quantitative PCR. The apoptotic assay and levels of intratesticular antioxidant enzymes were studied using ELISA. Using cART resulted in nuclear membrane breakdown, anomalies in the ultrastructural appearance of the germinal epithelium, and distortion of the progressive cellular growth. These changes were reduced with the co-administration of Naringenin. Co-administration of Naringenin limited the identified dysfunction of Sertoli cells as a sign of testicular toxicity from cART and this study suggests that as an adjuvant therapy, naringenin might help prevent testicular toxicity associated with long-term use of cART.

Keywords: testis; combination antiretroviral therapy; Naringenin; Sertoli cell, Stem cell factor, c-kit

INTRODUCTION

Highly Active Antiretroviral Therapy (HAART) in the form of Combination Antiretroviral Therapy (cART)is recommended for persons with HIV to reduce morbidity and prevent transmission of the virus to others. Unfortunately, cART often damages the testes and impair sperm production [1,2]. Spermatogenesis is an event that is controlled by several regulatory factors, including the interaction of the c-kit protein and the kit ligand-stem cell factor (SCF) [3]. The *c-kit* gene codes for a transmembrane tyrosine kinase receptor for the SCF protein. Germ cell proliferation, migration, and survival during the phases of sperm cell maturation are affected by SCF signaling via the c-Kit receptor, the expression, and function of which are crucial to successful reproduction [4]. Previous studies demonstrated that stimulation of the c-kit receptor by its ligand is essential for maintaining differentiated type A spermatogonia in the germinal epithelium of the testes [5]. In addition, abnormal expressions of SCF and c-kit have been linked to a distorted antioxidant balance and ultrastructural changes in the testes [6].

The two processes of steroidogenesis and sperm generation are straddled by the testis. Spermatogenesis is heavily reliant on oxygen, but the

testes are also extremely susceptible to the harmful effects of reactive oxygen metabolites [7]. Consequently, the testis produces a potent antioxidant system that includes both enzymatic and non-enzymatic elements. During the spermatogenesis process, the enzymatic component is activated. Currently, superoxide anion (O^{2-}) is formed by the high mitochondrial oxygen consumption of the germinal epithelium. O^{2-} is converted to hydrogen peroxide (H_2O_2) in the presence of superoxide dismutase (SOD). The formation of H_2O_2 prevents the formation of highly toxic hydroxyl radicals. The resulting H_2O_2 is also a powerful transmembrane oxidant that must be rapidly removed from the cell by the system to limit oxidative damage to lipids, proteins and DNA. H_2O_2 is removed by either catalase or glutathione peroxidase [8].

Several factors may perturb the smooth antioxidant balance in the testes. These factors cause a state of oxidative stress in the testes. Free radical damage is now considered the most important cause of testicular dysfunction in the pathogenesis of many male infertility. The causes range from varicocele [9], diabetes [10], testicular torsion [11], xenobiotic exposure (drug, pesticide, or carcinogen) [12,13] as well as idiopathic cases [14]. In addition, antiretroviral therapy has been linked with harmful structural changes in the testes, demonstrated by tubular degeneration and altered morphometric indices [1,2]. The mechanism of injury is, however, still unclear.

Naringenin is a bitter, colourless flavanone[15] found predominantly in grapefruit[16] and is a variety of fruits and herbs[17]. Naringenin is identified with its potent bioactive effects on human health in a wide range of beneficial ways. These include anti-inflammation[18], antioxidant [19], oestrogen activity modulator[20] as well as DNA protection and repair [1]. This study examined testicular ultrastructural abnormalities and expression of the *c-kit* gene and its ligand SCF following oral administration of cART and Naringenin.

MATERIALS AND METHODS

Adult male Sprague-Dawley (SD) rats between 200–220 g were obtained from the animal house of the Biomedical Resource Unit, University of KwaZulu-Natal, South Africa. They were housed in standard plastic cages (three rats/ cage) with dimensions of 30 cm long, 20 cm wide, and 13 cm high. Wood shavings were used for bedding in the cages. Animals were kept under controlled environmental conditions. They had free access to standard rat pellet food and clean water. HAART fixed-dose combination (FDC) containing efavirenz (EFV) 600 mg, emtricitabine (FTC) 200 mg, and tenofovir (TDF) 300 mg [TDF/FTC/EFV] was obtained from Pharmacare Ltd, Port Elizabeth, Republic of South Africa and was administered daily to rats (Adult Antiretroviral Therapy Guidelines 2014). The dose of FDC was adjusted according to animal weight using the human therapeutic dose equivalent (7.5/5/15 mg/kg) for the rat model.

The powdered form of Naringenin (95%) was bought from Sigma Aldrich Avengelee.

Thirty (30) adult male SD rats were randomly divided into six groups of 5 animals each. Group DW served as control and was given distilled water, H had the Fixed-Dose Combination FDC) of cART containing Tenofovir (TDF), Emtricitabine (FTC), and Efavirenz (EFV); N40 had Naringenin, 40 mg/kg, N80 was given Naringenin, 80 mg/kg. The last two groups- HN40 and HN80 had FDC of TDF/FTC/EFV and naringenin 40 mg/kg and 80mg/kg, respectively. All administrations were through the oral route and were done between 8:00 am and 10:00 am for ten weeks. Animals were weighed on alternate days for dose adjustments. The study followed the Guiding Principles in the Use of Animals in Toxicology, which the Society of Toxicology adopted in 1989. The Animal Research Ethical Committee approved this research of the University of KwaZulu-Natal (UKZN), South Africa (protocol reference number AREC/046/016D).

Animal Sacrifice and Collection of Samples

The SD rats were euthanized on day 70 under excess halothane anesthesia. The testes were excised, weighed, and processed for electron microscopy and molecular studies. Then, the cauda epididymides of each rat were excised and gently minced in 2 ml of normal saline. The resulting solutions were stored at -20 ℃.

RNA Extraction and cDNA Synthesis

The Zymo Research Quick-RNA™ Miniprep kit (Zymo Research U.S.A.) extracted the total RNA according to the manufacturer's instructions. Before RNA extraction, the tissues were homogenized in RNA lysis buffer. According to the manufacturer's instructions, cDNA synthesis was then done using the iScript cDNA Synthesis Kit (Bio-Rad, U.S.A.).

Real-time Polymerase Chain Reaction (PCR)

The Roche LightCycler 96 (Roche Diagnostics, Mannheim, Germany) was used for PCR amplification. The total reaction volume was 20 μL, made up of 2 μL of cDNA, 10 μL of ROCHE LightCycler SYBR green 1 master-mix (Roche Diagnostics, Mannheim, Germany), 4 μL of nuclease-free water, 2 μL each of forward and reverse primers at 20 μM concentration. The primers sequence used can be found below:

- Rat c-kit F TTCCTGTGACAGCTCAAACG

Rat c-kit R AGCAAATCATCCAGGTCCAG [21]

- Rat SCF F CAAAACTGGTGGCGAATCTT

  Rat SCF R GCCACGAGGTCATCCACTAT [21,22]

The thermal cycler parameters are 94 °C for 10 min, followed by 45 cycles of denaturing at 94°C for 15 seconds, annealing at 60 °C for 30 seconds, and extension at 72 °C for 30 seconds. In each was included a positive and negative control. All samples were analyzed in duplicate. The comparative Ct method ($2\text{-}\Delta\Delta Ct$) was used to compare cycle threshold (Ct) values (the number of cycles required for the fluorescent signal to cross the threshold) of the test groups to that of controls. A pool of cDNA from control samples was used to construct standard curves. In this study, glyceraldehyde-3-phosphate dehydrogenase (GAPDH) was used as the housekeeping gene, and Ct values of control, as well as test groups, were normalized to GAPDH [23].

Apoptosis Assay

The level of apoptosis on epididymal sperm samples was determined by assaying for caspase 8 using standardized Elabscience enzyme-linked immunoassay (ELISA) rat specific kits (catalog number E-EL-R0280).

Biochemical Estimation for Oxidative Enzyme Levels

One testis from each rat was homogenized using a Teflon homogenizer (Heidolph Silent Crusher M). The homogenates were centrifuged at 10,000g at 4ºC for 15 min. Homogenized tissues were used for catalase and glutathione peroxidase assay using standardized ELISA rat specific kits (catalog numbers: E-EL-R2456 and E-EL-R2491, respectively).

Ultrastructural Studies

One testis from each rat was cut into 1-mm cubes. These were fixed overnight at 4ºC in 3% glutaraldehyde in 0.1 M sodium cacodylate buffer (pH 7.4), and transferred to 0.1 M phosphate buffer (pH 7.2). The cells were postfixed in 1% osmium tetroxide in S-collidine, dehydrated in graded ethanols, transferred to propylene oxide, and embedded in Epon 812. The sample was further sectioned into ultrathin sections (75 nm) and contrasted with uranyl acetate and lead citrate. A transmission electron microscope was used to image detailed morphologic and compositional information [24].

Statistical Analysis

Statistical analysis was done using SPSS version 23 for windows. The data were calculated as mean ± SEM and presented as bar charts. The statistical significance of differences was evaluated by using a one-way analysis of variance (ANOVA) followed by Fisher's LSD procedure for multiple comparisons. $P < 0.05$ was considered statistically significant and $P < 0.01$, very significant.

RESULTS

Testicular Expression of SCF and c-kit

The expression of intratesticular SCF in the H group was significantly lower than in DW. Those of the naringenin-only treated groups [N40 and N80] were also lower than the control but not in significant amounts. The expressions in groups treated with both Naringenin and cART (HN40, and HN80) were not significantly different compared to the H group, as shown in figure 1 (a).

Testicular c-kit expression in the DW group was not significantly different from that of the H group. Higher expressions were observed in groups N40 and N80 than in the other groups. The minimum expressions were observed in groups HN40 and HN80. Significantly different observations existed between groups DW and HN80 and between HN80 and the naringenin-only groups (N40 and N80), as shown in figure 1(b).
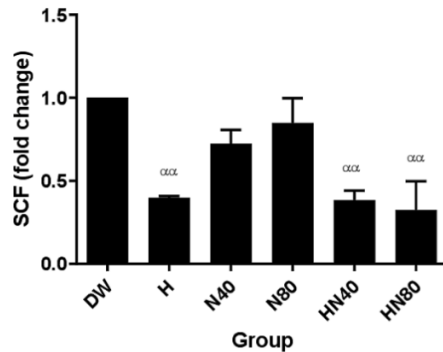
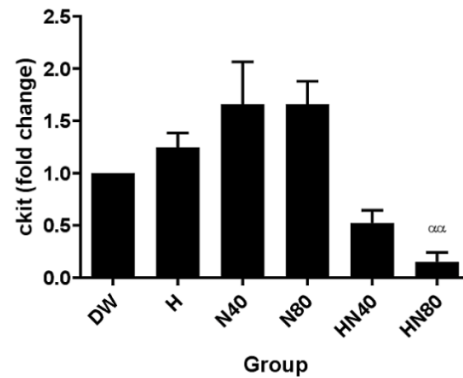Figure 1(a)   Figure 1(b)

Figure 1:   (a) Testicular SCF and (b) Testicular c-kit in groups DW (control), H (HAART), N40 (Naringenin 40 mg/kg), N80 (Naringenin 80 mg/kg), HN40 (HAART + Naringenin 40 mg/kg) and HN80 (HAART + Naringenin 80 mg/kg) after 10 weeks of treatment. Bars indicate mean±SD. and $^{\alpha\alpha}$ represents difference ($p<0.01$) between the group and DW group.

Apoptotic Assay

There was a significant reduction in the testicular caspase 8 in the Naringenin administered groups compared to control (DW) and HAART (H) groups. Levels in H were the highest with a significant difference when compared to N40 ($p=0.007$), N80 ($p=0.009$), and HN80 ($p=0.049$), as shown in Figure 2.
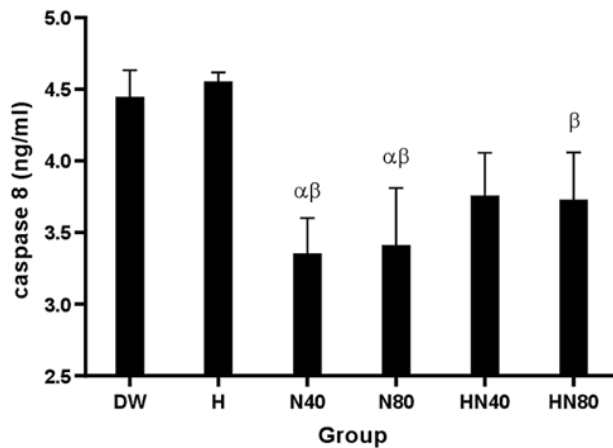

Figure 2:   Testicular caspase 8 in groups DW (control), H (HAART), N40 (Naringenin 40 mg/kg), N80 (Naringenin 80 mg/kg), HN40 (HAART + Naringenin 40 mg/kg) and HN80 (HAART + Naringenin 80 mg/kg) after 10 weeks of treatment. Bars indicate mean±SD. α represents significant difference ($p\leq0.05$) between the group and control, βrepresents significant difference between the group and P group ($p\leq0.05$).

Antioxidant Enzymes

The DW group displayed significantly higher levels of testicular glutathione peroxidase levels when compared to the H group. The levels observed in the N40 and N80 groups were higher than DW but not significantly. Catalase activity does not differ much in the DW and H groups. The N80 group showed a significantly higher level of testicular catalase activity than groups DW ($p=0.024$) and H ($p=0.003$) see figure 3 (a) and (b). The level in the HN40 was significantly higher than that of H ($p=0.019$).

(a)   (b)
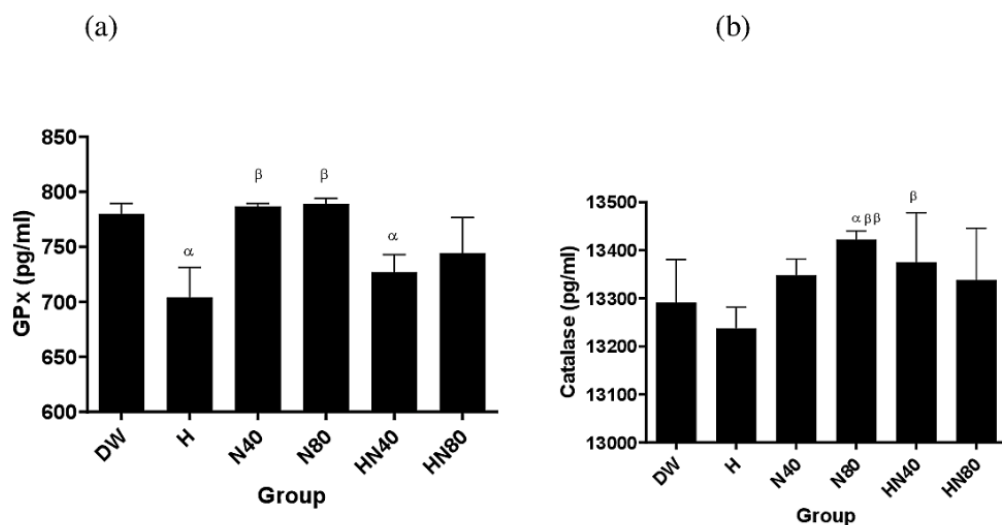

Figure 3: (a) Testicular glutathione peroxidase and (b) catalase in groups DW (control), H (HAART), N40 (Naringenin 40 mg/kg), N80 (Naringenin 80 mg/kg), HN40 (HAART + Naringenin 40 mg/kg) and HN80 (HAART + Naringenin 80 mg/kg) after 10 weeks of treatment. Bars indicate mean±SD. $^\alpha$ represents significant difference ($p<0.05$) between the group and control, $^\beta$ represents significant difference between the group and H group.

Ultrastructural Study

Group DW: Basal and ad luminal compartments and interstitium

The ultrastructure of the control group (DW) displays cells in the different stages of maturation. The early and late cellular stages of spermatogenesis presented a well-circumscribed nuclear membrane. The Sertoli cells displayed prominent nucleolus next to the myoid cells of the basement membrane with normal thickness. The primary spermatocytes appear rounded with large nuclei [figure 4 (a) - (d)]. The germinal epithelium depicting normal testicular architecture with an orderly progression of cells of the spermatogenic series indicates active spermatogenesis. Shown in figure 4(e) - (g) are the ad luminal compartments displaying round and elongating late spermatids surrounded by residual cytoplasm with several microtubules of the midpieces, suggesting multiple spermatozoa. Each piece depicts typical flagella axonemes composed of an array of microtubules containing nine doublets arranged radially around two single central ones. Mitochondria sheaths are seen in the middle pieces. Also observed are the lysosomes, ribosomes, and smooth endoplasmic reticulum.

The interstitium houses the interstitial cells of Leydig (Ly), with the nucleus having slight indentation and rich in euchromatin. A rim of heterochromatin lines the nuclear membrane. A large lymphatic vessel is seen traversing the interstitium. There was an abundance of mitochondria and lipid droplets suspended within the cytoplasm of the Leydig cell. Other organelles such as lysosomes and smooth endoplasmic reticulum are dispersed in the Leydig cell cytoplasm. [figure 4(h) - (i)].
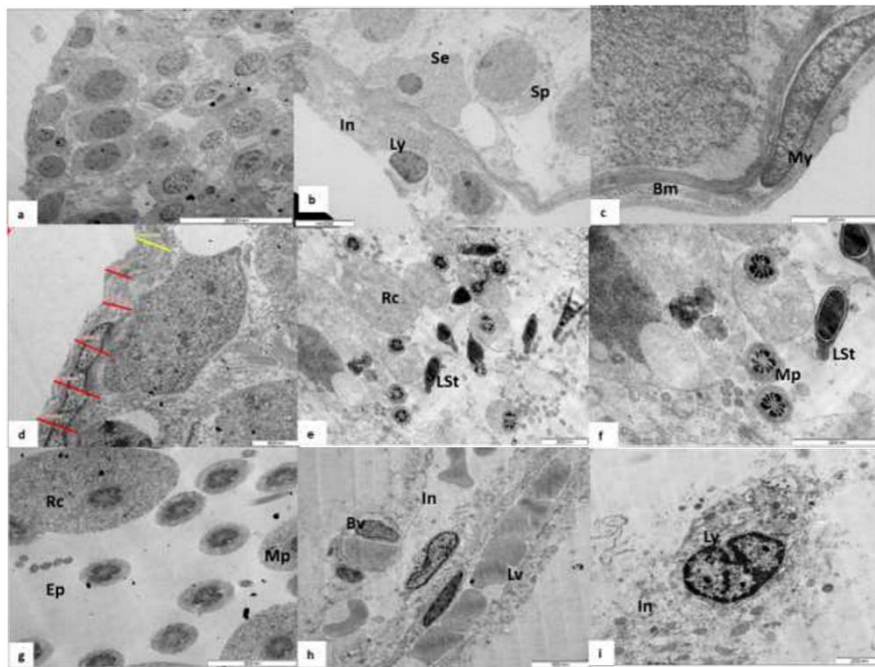
Figure 4: Ultrastructure of seminiferous tubule portion of group DW (control) depicts normal testicular architecture with an orderly progression of cells of the spermatogenic series showing the Sertoli cell (Se) with basement membrane (Bm), myoid cells (My), elongating late spermatid (St) midpiece (Mp), the interstitium (In) containing the interstitial cells of Leydig (Ly), blood vessel (Bv). Also seen is the lymphatic vessel (Lv). Scale bar for a, c, d, e, f, h, i is 2000 nm and 5000 nm for b,g

Group H: Basal and ad luminal compartments and interstitium

Figure 4 shows the electron micrographs of the ultrastructural of the seminiferous tubule portion of group H. This group has several ultrastructural abnormalities and disorganized germinal cells. There are alterations in the normal progression of cells in the germinal epithelium. The more matured cells belonging to the ad luminal compartment - early and late spermatids appear in the basal compartment. The outline of the basement membrane displays irregularities and increased thickness with hypertrophied myoid cells. There is a widening of the internuclear space between Sertoli cells, and there are scanty spermatogonic cells along with the basement membrane [figure 5(a) - (d)]. Seen are spermatocytes showing discontinuous nuclear membrane indicating degenerative processes in the cells. Also observed are abnormally formed spermatid heads. The axonemes of the midpieces appear disorganized in cross-section. The germinal epithelium appeared scanty, with spermatocytes surrounded by an abundance of residual cytoplasm suggestive of germ cell atrophy. Cross-section through the tail of the spermatozoa revealed axonemal defects in the form of lost organizations [figure 5(e) - (h)].

The interstitium presents Leydig cells appearing smaller with a reduced nuclear diameter and slight nuclear indentation [figure 5(i)]. In addition, there is less euchromatin within the nucleus, and the cytoplasm appeared scantier with fewer suspended organelles.
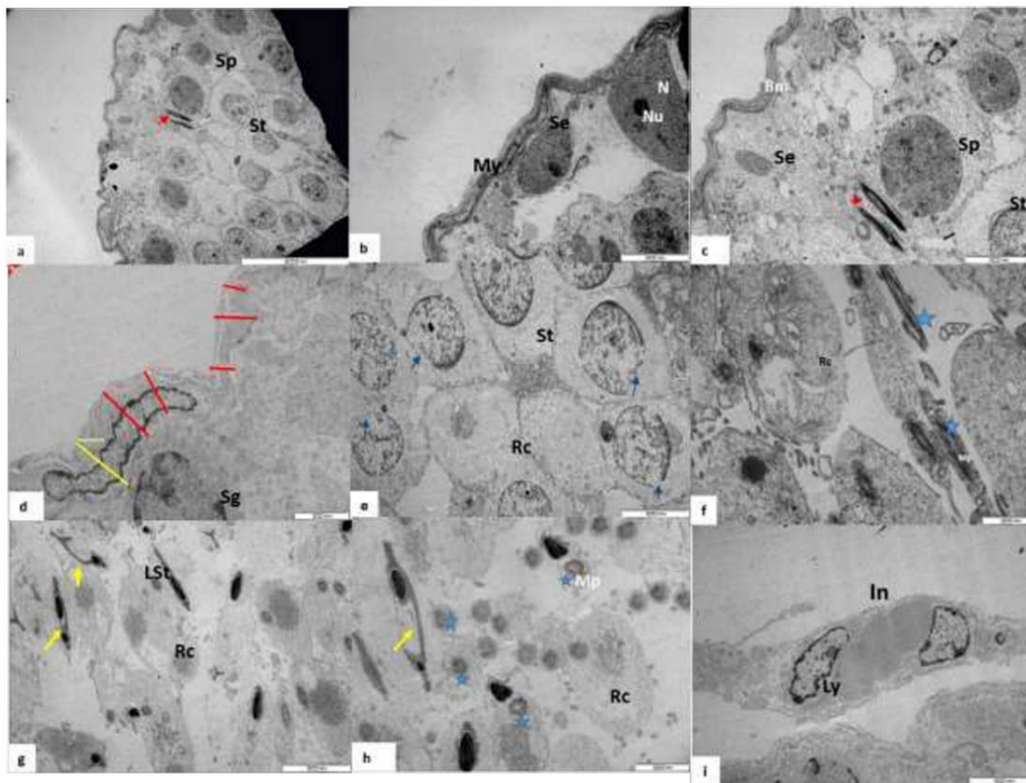
Figure 5: Ultrastructural micrograph of seminiferous tubule portion of group H highly active antiretroviral therapy (HAART only). This group has several ultrastructural abnormalities and disorganized germinal cells. Round Spermatid (St) and late spermatids (red arrow) basement membrane (Bm) and myoid cell (My), Sertoli cells (Se). Also, spermatid heads (yellow arrow) and midpiece (blue star) are surrounded by an abundance of residual cytoplasm (Rc). Scale bar for a, d, f, h is 2000 nm and for b, c, e, g, i is 5000 nm.

Group N40: Basal and ad luminal compartments and interstitium

Ultrastructure of the testes of rats in N40 (Naringenin 40 mg/kg) was similar to DW, showing the normal progression of cells of the spermatogenic series. The spermatogonia and Sertoli cells were resting on the basement membrane. The cells have well-circumscribed nuclei. The basement membrane demonstrates normal thickness and the myoid cells. [figure 6(a) - (c)]. The different stages of development of the spermatids were seen. The round spermatids and the late spermatids (LSt) were observed displaying normal appearance. The residual cytoplasms of the late spermatids were present close to the lumen, with the midpieces suspended within.

The nuclei appeared to be rich in euchromatin [figure 6(d) - (f)].

The Leydig cells were seen in the interstitium with slight nuclear indentations. The nucleus appeared large and rich in euchromatin. There was an abundance of cellular organelles suspended within the cytoplasm, including mitochondria and lipid droplets. Blood vessels were observed traversing the interstitium [figure 6(g) - (i)]. No vacuolation was observed.
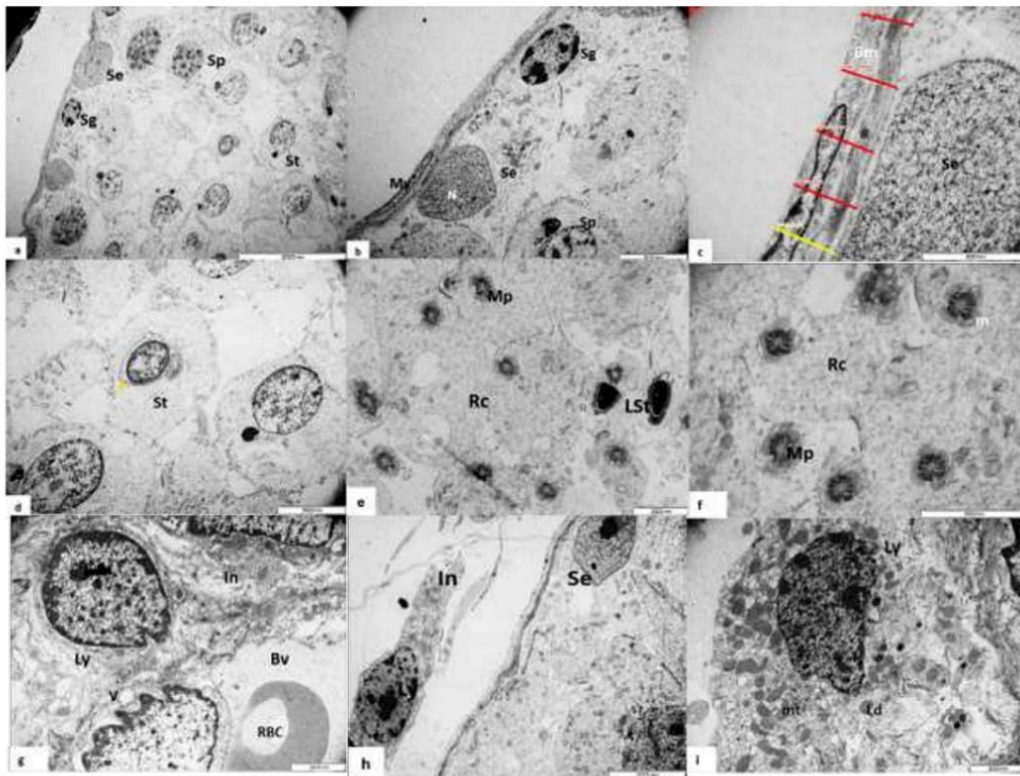
Figure 6: Ultrastructure of the testes of rats in N40 (Naringenin 40 mg/kg) The spermatogonia (Sg) and Sertoli cells (Se) spermatogonia (Sg), spermatocytes (Sp), nucleus (N) round spermatids (St), and the late spermatids (LSt), midpiece (Mp) Leydig cells (Ly), interstitium (In). Scale bar for a, c, e, f, g, i is 2000 nm and b, d, h are 5000 nm. Figure 6: Ultrastructure of the testes of rats in N80 (Naringenin 80 mg/kg). Spermatogonia (Sg), Sertoli cells (Se), nucleus (Nu), primary spermatocyte (Sp), ad luminal compartment (ALC), residual cytoplasm (Rc) and vacuoles (v), midpiece (g) The Leydig cells (Ly) are seen, interstitium (In), blood vessel (Bv). Scale bar for a, b, c, e, f, g, h, i is 2000 nm and d is 5000 nm.

Group N80: Basal and ad luminal compartments and interstitium

Electron sections of the testes of rats in N80 (Naringenin 80 mg/kg) show the normal progression of cells of the spermatogenic series. The spermatogonia and Sertoli cells are aligned along the basement membrane. Cells have a well-circumscribed nucleus and normal internuclear space. The basement membrane demonstrates normal thickness and myoid cells. Also seen are the primary spermatocytes [figure 7(a) - (d)]. The cross-section of the ad luminal compartment revealed a large population of spermatozoa tails close to the lumen showing midpieces and flagellum made up of the principal pieces and the end pieces. The axonemes of the pieces are well organized. Also seen are the residual cytoplasm and vacuoles accommodating the midpieces [figure 7(e) - (g)].

The Leydig cells (Ly) are seen in the interstitium. The nuclei are large and rich in euchromatin. In addition, the cells possess abundant mitochondria and lipid droplets within their cytoplasm. A large blood vessel containing red and white blood cells in the interstitium was observed [figure 7(h) - (i)]. Other cell types are observed within the interstitial tissue.
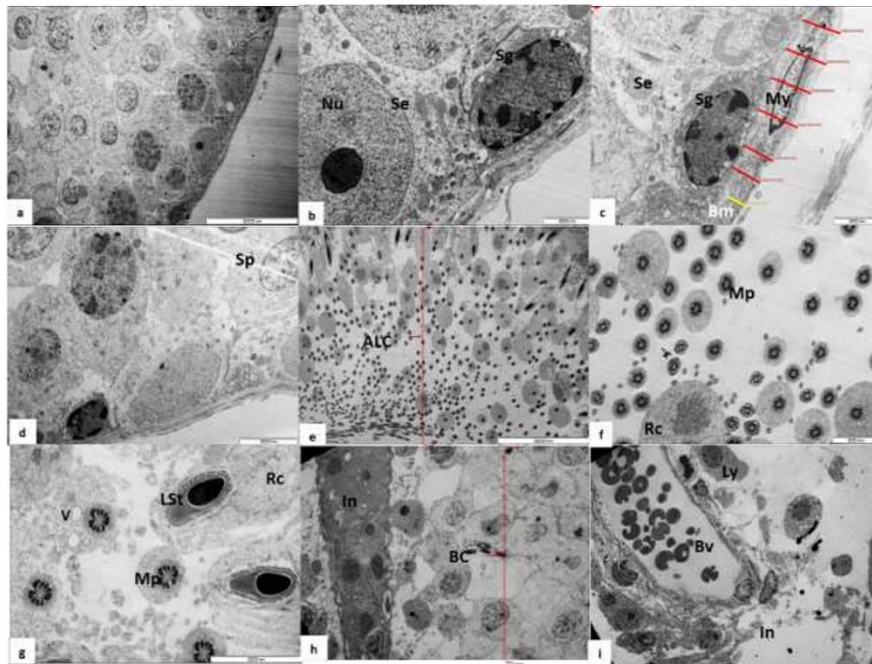
Figure 7: Ultrastructure of the testes of rats in N80 (Naringenin 80 mg/kg). Spermatogonia (Sg), Sertoli cells (Se), nucleus (Nu), primary spermatocyte (Sp), ad luminal compartment (ALC), residual cytoplasm (Rc) and vacuoles (v), midpiece (g) The Leydig cells (Ly) are seen, interstitium (In), blood vessel (Bv). Scale bar for a, b, c, e, f, g, h, i is 2000 nm and d is 5000 nm.

Group HN40: *Basal and ad luminal compartments and interstitium*

Observation from testes of the HN40 group presented some improvement in the ultrastructural appearance compared to the H group. Electron sections show Sertoli and spermatogonic cells lined along the basement membrane. The myoid cells of the basement membrane are closely related to the spermatogonic cells. There is a slight thickening of the basement membrane. The primary spermatocytes present with some degenerative changes in the nuclear membrane [figure 8(a) - (f)]. The cross-section of the tails of late spermatids shows the midpiece, principal piece, and end piece. There are a few midpieces with disorganized axonemes and abnormal spermatid heads [figure 8(g) - (h)].

The Leydig cells appear with deep nuclear indentations. Nuclei present with normal chromatin condensations. Cytoplasmic organelles are seen suspended. Blood vessels are seen traversing the interstitium. Improvement in observations from the H group was noted [figure 8(i)].
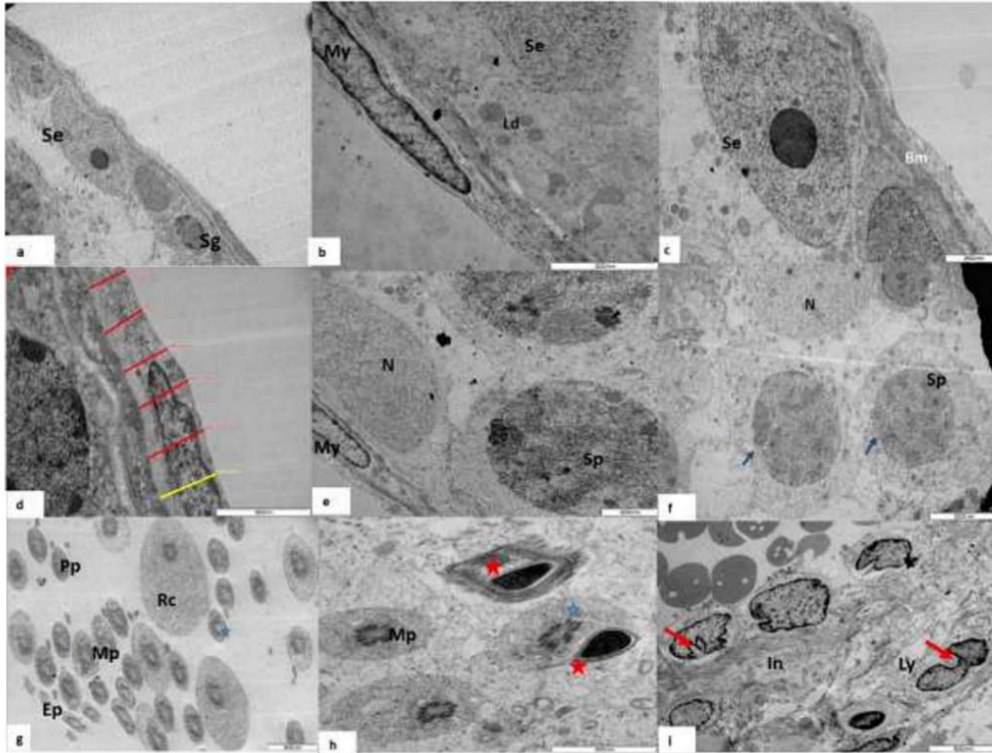
Figure 8: Ultrastructure of testes of group HN40. Sertoli (Se), spermatogonic cells (Sg), basement membrane (Bm), spermatogonic cells (Sg), degenerative changes in the nuclear membrane (blue arrow), midpiece (Mp), principal piece, and endpiece (Ep), there are a few midpieces with disorganized axonemes (blue star), abnormal spermatid heads (red star). Scale bars for a, b, c, d, e, g, h are 2000 nm and 5000 nm for f, and i.

Group HN80: *Basal and ad luminal compartments and interstitium*

Ultrastructure of the testes of group HN80 reveals the normal progression of cells of the spermatogenic series. The Sertoli and Spermatogonic cells lie on the basement membrane with myoid cells in the adjacent basement membrane. The basement membrane has a relatively straight outline with slight thickening [figure 9(a) - (d)]. Round spermatids display acrosomal cap and occasional degeneration of nuclear membrane. The Late spermatids in the process of spermiation are observed. The lumen of the seminiferous tubule contains a cross-section of tails showing abundant midpieces and principal pieces. There is some residual cytoplasm around the midpieces. Occasional abnormal forms in the late spermatids were observed [figure 9(e) - (h)].

Leydig cells lie amidst scanty cytoplasmic organelles. The cells displayed reduced chromatin condensation, and no vacuoles were observed. There is a slight nuclear indentation in the Leydig cells [figure 9(i)].
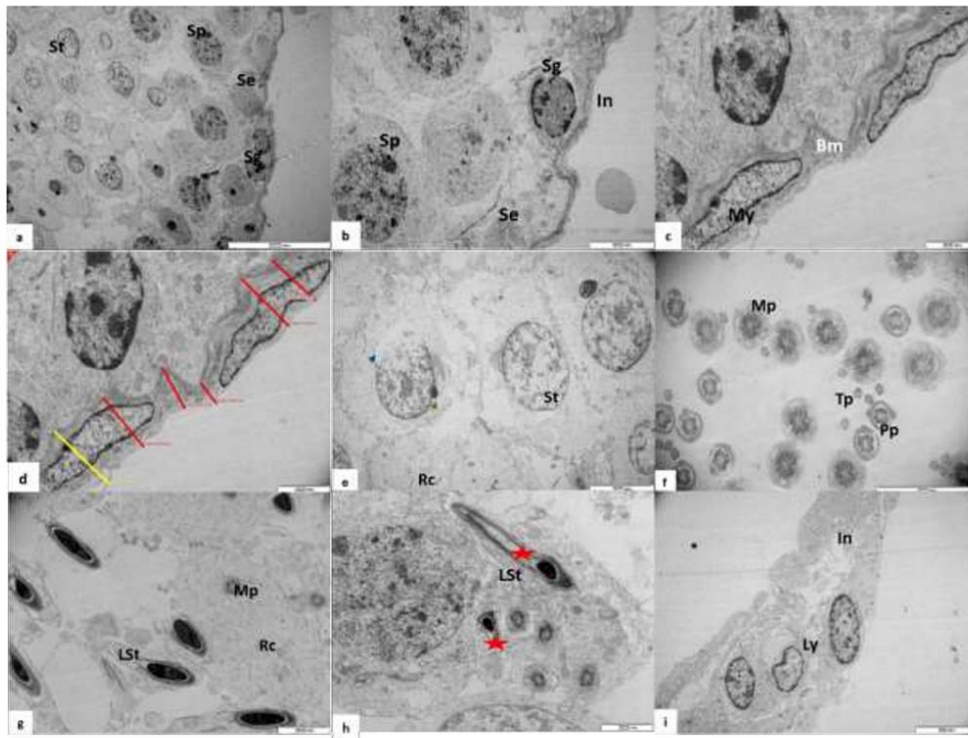
Figure 9: Ultrastructure of testes of group HN80. The Sertoli (Se), Spermatogonic (Sg) cells, basement membrane (Bm). Round spermatids (St), midpieces (Mp), and the principal pieces (Pp). (g) Late spermatids (LSt), residual cytoplasm (Rc) around the midpiece (Mp), abnormal forms in the late spermatids (red star), Leydig cells (Ly, interstitium (In). Scale bars for (a), (c), (d), (f), (g), (h) is 2000 nm and 5000 nm for (b), (e), (i).

DISCUSSION

Combination Antiretroviral Therapy (cART) is recommended for all individuals with HIV, regardless of CD4 cell count, to reduce the morbidity and mortality associated with HIV infection and prevent transmission. Commencement of cART, however, means lifelong use despite the organotoxic properties of the regimen. This study describes antiretroviral therapy-induced alterations in testicular ultrastructure and antioxidant activity of adult male Sprague Dawley rats and evaluates the possible protective role of Naringenin.

The Spermatogenic process is highly dependent on the SCF/c-kit system. The *c-kit* gene encodes a transmembrane tyrosine kinase receptor for the SCF protein. Activation of c-kit signaling has been found to mediate cell survival, migration, and proliferation depending on the cell type. Signaling from c-Kit is central to successful fertility, normal hematopoiesis, amongst others [25,26]. The study revealed a reduced expression of both SCF and c-kit in the cART-treated groups. This reduction may explain the scanty spermatogenic cells found along the basement membrane and alterations in the normal progression of cells in the germinal epithelium. The expression of

c-kit was higher in the Naringenin-only groups; however, co-administration of cART and Naringenin could not ameliorate the distortion in the expressions of either SCF or c-kit. The elevation of c-kit expression has been linked with the commitment of spermatogonial stem cells to differentiate[27]. It has been shown that the disruption of the SCF/c-kit system displayed a crucial impact on germ cell survival and male fertility [28].

Apoptosis is a fundamental process of maintaining tissue homeostasis, removing damaged cells, and reprocessing cellular constituents. Caspases are a group of cysteine proteases that act as apoptosis initiators to dismantle cellular structures proteolytically. They maintain homeostasis by removing damaged cells and reprocessing cellular constituents for further differentiation. Activated caspase-8 propagates the apoptotic signal either by directly cleaving and activating downstream caspases or by cleaving BH3 interacting-domain death agonist, a pro-apoptotic member of the Bcl-2 protein family [29]. This study showed that the level of caspase 8 following administration of HAART was not significantly increased in the testes. However, a study has shown that antiretroviral therapy can induce apoptosis in some body organs [30]. Caspase 3 levels

were noticed to be increased with the use of HAART [31], this was not observed in the present study. Administration of Naringenin further reduced the levels of intratesticular caspase 8, suggesting reduced cellular damage in the setting of a potent bioactive flavonoid.

In this study, administration of HAART was associated with a reduction in the activity of testicular antioxidant enzymes. The testicular activity of glutathione peroxidase increased significantly in the naringenin-only groups compared to the other experimental groups, particularly in the HAART group. *In vivo* studies in humans however reported increased oxidative stress and caused mitochondrial alterations in HIV patients following long-term treatment with HAART[32]. The co-administration of Naringenin and HAART restored enzyme activity at a higher dose of Naringenin. Similar findings were observed with the activity of catalase. Catalase activity was highest with a high dose of Naringenin; however, the enzyme activity was only restored to values higher than that of control using low dose naringenin. The improved activity of antioxidant enzymes in tissues may explain the earlier identified free radical scavenging properties of Naringenin as previously described [33,34]. Similar to Naringenin, Rutin, a citrus flavonoid, has been shown to increase testicular Glutathione peroxidase and Glutathione activities in a dose-dependent manner. [35,36].

This study revealed alteration of the normal ultrastructure of the testes with the use of cART. The irregular contouring and thickening of the basement membrane resulted from cellular infiltration of the basement membrane. The occurrence of tubular degeneration has been linked to the basement membrane's thickening, thereby hindering metabolic exchange between the germinal epithelium and the interstitium [37]. This subsequently leads to gonadotrophin deficiencies [38,39]. Similar pathology in other atrophic testes with a different etiology are consistent findings [40]. The altered exchange of materials within the testicular tissue further induces basement membrane infiltration and further thickening.

Aging is another situation related to a convoluted and thickened basement membrane [41]. An increase in the expression of basement membrane genes has been implicated in this process. This usually precedes atrophy of the seminiferous tubules [41]. Both the seminiferous tubule and the myoid cells are required for appropriate deposition of basement membrane in the testes; an abnormality in the basement membrane may suggest a malfunction of either the myoid cell or Sertoli cell [41].

Germ cell injury has been identified as the most critical morphologic event underlying testicular dysfunction following the administration of cytotoxic compounds. These morphologic changes usually explain the mechanism of action of the gonadotoxic agent [42,43]. The normal progression of the cells in the seminiferous germinal epithelium was altered following the use of cART. This was evidenced by elongating spermatids being retained and resorbed into basilar Sertoli cell cytoplasm within the basal compartment. The spermatogonic cells along the basement membrane were observed to be scanty following the use of cART. However, the Sertoli cells seem unaffected; there was an associated reduction in the population of primary spermatocytes. In addition, the spermatocytes and round spermatids displayed an incomplete nuclear membrane. This suggests some degenerative processes ongoing within the cell. Exposure to environmental toxicants, mostly chemical substances that target the reproductive organs, can either directly disrupt the endocrine system or induce changes in the organization. This results in the malfunctioning of the cellular components of the seminiferous tubules. The morphological changes described have been associated with impaired Sertoli cell function [44]. Other studies that described the morphologic changes in the rat testes, such as spermatid retention and degeneration of cells, linked it with decreased intratesticular testosterone levels [45,46].

The spermatogonia are a group of mitotically active cell cohorts capable of self-renewal and differentiation into mature sperm cells. Being the mitotic component of spermatogenesis and the primary germ cell type not protected by the blood-testis barrier, spermatogonia are known to be the most vulnerable to toxic effects [47,48]. However, stem cell spermatogonia are known to be less sensitive to the effects of gonadotoxic compounds; it thus seems logical to hypothesize that injury to the testes may be reversible following cessation of exposure through seminiferous epithelial reconstitution from surviving stem cell spermatogonia [49]. This is, however, dependent on the class of toxic agents as there exists much variability across different compounds.

The basic patterns of reaction to xenobiotic-induced injury to the testis described by Vidal *et al.*, re expressed using HAART [44]. The spermatocytes and older cell types in the germinal epithelium are spared, leaving the Sertoli and spermatogonic cells to face the brunt of the injury. This is because the spermatocytes and spermatids are protected by the blood-testis barrier[50]. The toxic agent will have to circumvent this barrier to affect them. However, extended exposures to toxicants can cause maturation depletion, resulting in the loss of more mature germ cell layers. It has also been observed that Sertoli cell injury is expressed by loss of function rather than Sertoli cells themselves.

The many roles that Sertoli cells play in spermatogenesis are reflected in various morphologic manifestations associated with Sertoli cell toxicity. An impaired Sertoli cell function expresses as germ cell degeneration. Similarly, degeneration of the seminiferous epithelium may either present as endocrine toxicity or direct germ cell injury following penetration of the toxic compound through the blood-testis barrier [44].

The co-administration of Naringenin proved beneficial. The normal cellular progression was observed, and cells of the spermatogenic series were well represented; however, there were occasional defects in the continuity of the nuclear membrane. This therapeutic potential associated with the use of high-dose Naringenin is in tandem with earlier observations[1]. Kwatra et al revealed that naringin usage, a closely related flavonoid modified the behavior alternation in Doxorubicin-treated rats, oxidative stress, proinflammatory cytokines, mitochondrial dysfunction, and improved monoamine contents in brain hippocampus of rats [51]. The addition of Naringenin to oseltamivir treatment improved the neurofunctions of the brain through improving the Y maze task and reducing the pathophysiological effect of oseltamivir. This was attributed to increasing total antioxidant capacity, brain fatty acid-binding proteins FABP7 and Ca-ATPase, and reducing oxidative [19]. In the same study, Naringenin was proposed to have reduced total nitric oxide, total oxidant capacity, and total cytochrome P450 (CYP450) contents [19].

Some studies have proposed an improvement in antioxidant activity. For example, the supplementation of Naringenin and its synthetic derivative enhanced antioxidant enzyme activities of erythrocyte and liver in high cholesterol-fed rats by enhancing the antioxidant defence system [52]. In cisplatin-naringenin combined treated rats, the activities of superoxide dismutase, glutathione peroxidase, and catalase were significantly increased [34].

Naringenin has also been regarded as a chelating agent capable of binding to toxic metal ions to form complex structures which are easily eliminated from intracellular or extracellular spaces. Cavia-Saiz et al. revealed that Naringenin acts as an active chelator of metallic ions and inhibitor of the enzyme xanthine oxidase. These ameliorative effects of Naringenin may be attributed to its chemical structure. The hydroxyl groups present can donate electrons and mop up generated free radicals from the altered oxidative status, restoring the testes' oxidant-antioxidant balance. This provides an insight into the mechanism of the gonadotoxic effect of antiretroviral therapy. Ranawat et al. revealed opposing views when Naringenin was administered intraperitoneally to mice. They suggested that Naringenin may also act as a pro-oxidant in a dose-dependent fashion despite being a potent antioxidant. Hence, causing damaging effects in the testes observed as decreasing sperm motility and concentration and inducing alterations in testicular histomorphology [53]. This variance can be attributed to the difference in the route of administration used. Additionally, the naringenin vehicle used in the study, Dimethyl sulfoxide, exhibits a range of pharmacological activity, including the ability to penetrate biological membranes increasing the concentration of pharmacological agents within the tissue.

Conclusion

The present study reports that cART-induced ultrastructural changes in the testicular tissue due to Sertoli cell dysfunction and altered expression of the c-kit ligand system in the testes of adult rats. Some restoration of structure and function were achieved with Naringenin, therefore researchers suggest that it could be a useful adjuvant in the treatment of HIV patients, especially those desirous of future fertility.

Acknowledgments

REFERENCES

1. Adana MY, Akang EN, Peter AI, Jegede AI, Naidu EC, Tiloke C, et al. Naringenin attenuates highly active antiretroviral therapy-induced sperm DNA fragmentations and testicular toxicity in Sprague-Dawley rats. Andrology. 2018;6(1):166-175.
2. Azu OO, Naidu EC, Naidu JS, Masia T, Nzemande NF, Chuturgoon A, et al. Testicular histomorphologic and stereological alterations following short-term treatment with highly active antiretroviral drugs (HAART) in an experimental animal model. Andrology. 2014;2(5):772-779.
3. Joshi M, Singh RJGoMIAC-BGfC. Molecular Regulation of Sperm Production Cascade. 2020:19-37.
4. Sandlow JI, FENG HL, Cohen MB, Sandra A. Expression of c-KIT and its ligand, stem cell factor, in normal and subfertile human testicular tissue. Journal of Andrology. 1996;17(4):403-408.

5. Ohta H, Yomogida K, Dohmae K, Nishimune YJD. Regulation of proliferation and differentiation in spermatogonial stem cells: the role of c-kit and its ligand SCF. Development 2000;127(10):2125-2131.

6. Lu X, Liu J, Yin H, Ding C, Wang Y, Zhang F et al. Effects of liver-regulating herb compounds on testicular morphological and ultrastructural changes in varicocele rats through SCF/C-KIT pathway. Andrologia 2020;52(9):e13658. doi:https://doi.org/10.1111/and.13658

7. Chen H, Liu J, Luo L, Baig MU, Kim J-M, Zirkin BR. Vitamin E, aging and Leydig cell steroidogenesis. Experimental Gerontology. 2005;40(8):728-736.

8. Kehinde EO, Anim JT, Mojiminiyi OA, Al-Awadi F, Shihab-Eldeen A, Omu AE et al. Allopurinol provides long-term protection for experimentally induced testicular torsion in a rabbit model. BJU International. 2005;96(1):175-80. doi:10.1111/j.1464-410X.2005.05590.x

9. Taghizadeh L, Eidi A, Mortazavi P, Rohani AH. Effect of selenium on testicular damage induced by varicocele in adult male Wistar rats. Journal of Trace Elements in Medicine and Biology. 2017;44:177-185.

10. Ostovan F, Gol A, Javadi A. Investigating the effects of Citrullus colocynthis pulp on oxidative stress in testes and epididymis in streptozotocin-induced diabetic male rats. International Journal of Reproductive BioMedicine. 2017;15(1):41.

11. Mirhoseini M, Amiri FT, Malekshah AAK, Gatabi ZR, Ghaffari E. Protective effects of melatonin on testis histology following acute torsion-detorsion in rats. International Journal of Reproductive BioMedicine. 2017;15(3):141.

12. Lovato FL, De Oliveira CR, Adedara IA, Barbisan F, Moreira KL, Dalberto M et al. Quercetin ameliorates polychlorinated biphenyls-induced testicular DNA damage in rats. Andrologia. 2016;48(1):51-58.

13. Adedara IA, Abolaji AO, Odion BE, Omoloja AA, Okwudi IJ, Farombi EO. Redox status of the testes and sperm of rats following exposure to 2, 5-hexanedione. Redox Report. 2016;21(6):239-247.

14. Saleh RA, Agarwal A, Nada EA, El-Tonsy MH, Sharma RK, Meyer A et al. Negative effects of increased sperm DNA damage in relation to seminal oxidative stress in men with idiopathic and male factor infertility. Fertility and Sterility. 2003/06/01/ 2003;79(Supplement 3):1597-1605. doi:https://doi.org/10.1016/S0015-0282(03)00337-6

15. Abe K. Studies on taste: molecular biology and food science. Bioscience, biotechnology, and biochemistry. 2008:0806060899-0806060899.

16. Felgines C, Texier O, Morand C, Manach C, Scalbert A, Régerat F et al. Bioavailability of the flavanone naringenin and its glycosides in rats. Am J Physiol Gastrointest Liver Physiol 2000;279(6):G1148-G1154.

17. Yanez JA, Andrews PK, Davies NM. Methods of analysis and separation of chiral flavonoids. Journal of Chromatography B 2007;848(2):159-181.

18. Maatouk M, Elgueder D, Mustapha N, Chaaban H, Bzéouich IM, Loannou I et al. Effect of heated naringenin on immunomodulatory properties and cellular antioxidant activity. Cell Stress Chaperones 2016;21(6):1101-1109.

19. Hegazy HG, Ali EHA, Sabry HA. The neuroprotective action of naringenin on oseltamivir (Tamiflu) treated male rats. The Journal of Basic & Applied Zoology. 2016;77:83-90. doi:http://doi.org/10.1016/j.jobaz.2016.12.006

20. Diamanti-Kandarakis E, Bourguignon JP, Giudice LC, Hauser R, Prins GS, Soto AM et al. Endocrine-disrupting chemicals: an Endocrine Society Scientific Statement. 2009;30(4):293-342.

21. Nurmio M, Kallio J, Toppari J, Jahnukainen K. Adult reproductive functions after early postnatal inhibition by imatinib of the two receptor tyrosine kinases, c-kit and PDGFR, in the rat testis. Reproductive Toxicology. 2008;25(4):442-446.

22. Kazutaka S, Winnall WR, Muir JA, Hedger MP. Regulation of Sertoli cell activin A and inhibin B by tumour necrosis factor α and interleukin 1α: Interaction with follicle-stimulating hormone/adenosine 3′, 5′-cyclic phosphate signalling. Molecular and Cellular Endocrinology. 2011;335(2):195-203.

23. Zainuddin A, Chua KH, Rahim NA, Makpol SJBMB. Effect of experimental treatment on GAPDH mRNA expression as a housekeeping gene in human diploid fibroblasts. BMC Molecular Biology. 2010;11:1-7.

24. Hayat ME. Basic techniques for transmission electron microscopy. Elsevier; 2012.

25. Lennartsson J, Rönnstrand L. Stem Cell Factor Receptor/c-Kit: From Basic Science to Clinical Implications. Physiological Reviews. 2012;92(4):1619-1649. doi:10.1152/physrev.00046.2011

26. Keshet E, Lyman SD, Williams DE, Anderson DM, Jenkins NA, Copeland NG et al. Embryonic RNA expression patterns of the c-kit receptor and its cognate ligand suggest multiple functional roles in mouse development. The EMBO Journal.

1991;10(9):2425-2435. doi:10.1002/j.1460-2075.1991.tb07782.x

27. Schrans-Stassen BH, van de Kant HJ, de Rooij DG, van Pelt AM. Differential expression of c-kit in mouse undifferentiated and differentiating type A spermatogonia. Endocrinology. 1999;140(12):5894-5900.

28. Qin Q, Liu J, Ma Y, Wang Y, Zhang F, Gao S et al. Aberrant expressions of stem cell factor/c-KIT in rat testis with varicocele. Journal of the Formosan Medical Association 2017;116(7):542-548. doi:https://doi.org/10.1016/j.jfma.2016.09.001

29. Kruidering M, Evan GI. Caspase-8 in apoptosis: the beginning of "the end"? IUBMB Life. 2000;50(2):85-90.

30. Apostolova N, Gomez-Sucerquia L, Moran A, Alvarez A, Blas-Garcia A, Esplugues J. Enhanced oxidative stress and increased mitochondrial mass during Efavirenz-induced apoptosis in human hepatic cells. British Journal of Pharmacology. 2010;160(8):2069-2084. doi:10.1111/j.1476-5381.2010.00866.x

31. Hamed M, Akhigbe RJHR. P-002 Zinc restores testicular integrity and function in HAART-treated male Wistar rats via modulation of Nrf2/NFkB pathway and downregulation of caspase 3 signaling. Human Reproduction 2022;37(Supplement_1):deac107. 002.

32. Ikekpeazu JE, Orji OC, Uchendu IK, Ezeanyika LUJCcp. Mitochondrial and oxidative impacts of short and long-term administration of HAART on HIV patients. Curr Clin Pharmacol 2020;15(2):110-124.

33. Zbarsky V, Datla KP, Parkar S, Rai DK, Aruoma OI, Dexter DT. Neuroprotective properties of the natural phenolic antioxidants curcumin and naringenin but not quercetin and fisetin in a 6-OHDA model of Parkinson's disease. Free Radical Research. 2005;39(10):1119-1125.

34. Badary OA, Abdel-Maksoud S, Ahmed WA, Owieda GH. Naringenin attenuates cisplatin nephrotoxicity in rats. Life Sciences. 2005;76(18):2125-2135.

35. Abarikwu SO, Olufemi PD, Lawrence CJ, Wekere FC, Ochulor AC, Barikuma AM. Rutin, an antioxidant flavonoid, induces glutathione and glutathione peroxidase activities to protect against ethanol effects in cadmium-induced oxidative stress in the testis of adult rats. Andrologia. 2017;49(7):e12696. doi:10.1111/and.12696

36. Khan RA, Khan MR, Ahmed M, Shah MS, Rehman SU, Khan J et al. Effects of Rutin on Testicular Antioxidant Enzymes and Lipid Peroxidation in Rats. Indian Journal Of Pharmaceutical Education And Research. 2017;51(3):412-417.

37. Amat P, Paniagua R, Montero J. Seminiferous tubule degeneration in human cryptorchid testes. Journal of Andrology. 1985;6(1):1-9.

38. Hadziselimović F. Cryptorchidism. Ultrastructure of normal and cryptorchid testis development. Advances in Anatomy, Embryology, and Cell Biology. 1977;53(3):3-71.

39. Hadžiselimović F. Pathogenesis and treatment of undescended testes. European Journal of Pediatrics. 1982;139(4):255-265.

40. Neaves BW. The blood-testis barrier. The Testis. 1977;4:126-162

41. Richardson LL, Kleinman HK, Dym M. The effects of aging on basement membrane in the testis. Journal of Andrology. 1995;16(2):118-126.

42. Yuksel A, Bildik G, Senbabaoglu F, Akin N, Arvas M, Unal F et al. The magnitude of gonadotoxicity of chemotherapy drugs on ovarian follicles and granulosa cells varies depending upon the category of the drugs and the type of granulosa cells. Human Reproduction. 2015;30(12):2926-2935.

43. Gutierrez JC, Hwang K. The toxicity of methotrexate in male fertility and paternal teratogenicity. Expert Opinion on Drug Metabolism & Toxicology. 2017;13(1):51-58.

44. Vidal JD, Whitney KM. Morphologic manifestations of testicular and epididymal toxicity. Spermatogenesis. 2014/03/04 2014;4(2):e979099. doi:10.4161/21565562.2014.979099

45. Beardsley A, O'Donnell L. Characterization of Normal Spermiation and Spermiation Failure Induced by Hormone Suppression in Adult Rats1. Biology of Reproduction. 2003;68(4):1299-1307. doi:10.1095/biolreprod.102.009811

46. Troiano L, Fustini MF, Lovato E, Frasoldati A, Malorni W, Capri M et al. Apoptosis and spermatogenesis: evidence from an in vivo model of testosterone withdrawal in the adult rat. Biochemical and Biophysical Research Communications. 1994;202(3):1315-1321.

47. Meistrich ML. Critical components of testicular function and sensitivity to disruption. Biology of Reproduction. 1986;34(1):17-28.

48. McAbee KE, Pendergraft SS, Atala A, Bishop C, Sadri-Ardekani H. Effect of Environmental Toxins on Spermatogonial Stem Cells. Bioenvironmental Issues Affecting Men's Reproductive and Sexual Health. Elsevier; 2018:53-70.

49. Roeser HP SA, Smith AJ. Testicular damage due to cytotoxic drugs and recovery after cessation of therapy. Aust N Z J Med 1978;8:250-4.

50. Haverfield JT, Meachem SJ, Nicholls PK, Rainczuk KE, Simpson ER, Stanton PG. Differential Permeability of the Blood-Testis Barrier During Reinitiation of Spermatogenesis in Adult Male Rats. Endocrinology. 2014;155(3):1131-1144. doi:10.1210/en.2013-1878

51. Kwatra M, Jangra A, Mishra M, Sharma Y, Ahmed S, Ghosh P et al. Naringin and sertraline ameliorate doxorubicin-induced behavioral deficits through modulation of serotonin level and mitochondrial complexes protection pathway in rat hippocampus. Neurochemical Research. 2016;41(9):2352-2366.

52. Lee MK, Bok SH, Jeong TS, Moon SS, Lee SE, Park YB et al. Supplementation of naringenin and its synthetic derivative alters antioxidant enzyme activities of erythrocyte and liver in high cholesterol-fed rats. Bioorganic & Medicinal Chemistry. 2002;10(7):2239-2244.

53. Ranawat P, Bakshi N. Naringenin; a bioflavonoid, impairs the reproductive potential of male mice. Toxicology Mechanisms and Methods. 2017;27(6):417-27.